

# Geant4 Simulations of Machine-Induced Background in a TPC

Adrian Vogel\*

2007-09-11

## Abstract

I present simulation results for machine-induced backgrounds in a TPC, which is foreseen as the main tracker of the LDC detector. Using Guinea-Pig as a particle generator and Mokka as a full detector simulation, background occupancies and space charges are estimated. Some special attention is paid to neutrons. [1]

## 1 Backgrounds at the ILC

Even though the ILC is expected to provide a very clean experimental environment, its operation will not be perfectly background-free. A main source of backgrounds are electron-positron pairs which are created during the collision of the very strongly-focussed bunches. Due to the high space charge, the particles in the bunches can emit “beamstrahlung” photons [2] which can in turn scatter and create electron-positron pairs with typical energies in the GeV range. Other background sources are either supposed to be negligible (such as the beam dump or synchrotron radiation from the final focus) or have to be studied in further detail (e. g. the beam halo or losses in the extraction line).

In the order of  $10^5$  pairs are created per bunch crossing, but they very rarely reach the TPC directly because of their forward boost and the focussing effect of the strong magnetic field. Instead, they hit the forward calorimeters (mostly the BeamCal, which is in fact designed to observe the spatial distribution of the pairs) and the magnets of the beam delivery and/or the extraction line. There they create charged particles and photons in large quantities, and also neutrons can be released by photonuclear reactions.

Some of these shower products are backscattered, and while most of the charged particles will be confined to the innermost parts of the detector by the magnetic field, photons and neutrons can easily reach the TPC. The chamber gas can then be ionised through photon conversion, Compton scattering, and – in the case of neutrons – recoiling protons, provided that the quencher gas contains hydrogen.

---

\*DESY FLC, 22603 Hamburg, Germany, [adrian.vogel@desy.de](mailto:adrian.vogel@desy.de)

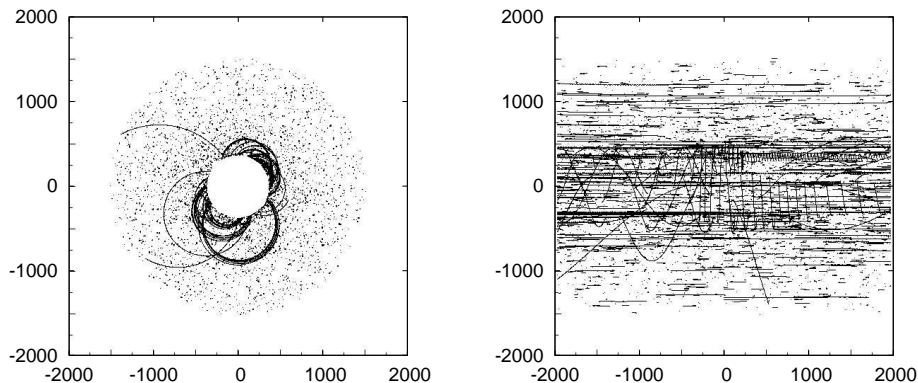


**Figure 1:** Front view (left) and side view (right) of Mokka hits from 100 bunch crossings

## 2 Simulation Tools

### 2.1 Guinea-Pig – Particle Generator

Guinea-Pig [3] is used to simulate the beam-beam interaction. Given a set of beam parameters (energy, bunch sizes, emittances, bunch charge, etc.), Guinea-Pig writes out the electron-positron pairs which are created in one bunch crossing. For this talk, 100 bunch crossings with nominal ILC beam parameters [4] at  $\sqrt{s} = 500$  GeV are used.

### 2.2 Mokka – Full Detector Simulation

The Geant4-based application Mokka [5] is used for a full simulation of the detector. The geometry corresponds to the “LDC version 2” [6], featuring a TPC with a sensitive volume of  $371 \text{ mm} < r < 1516 \text{ mm}$  and  $|z| < 1970 \text{ mm}$ . In the forward region there is a rather large distance of 1080 mm between LumiCal and BeamCal, which helps in shielding backscatterers from the BeamCal and therefore reduces the number of photons being able to reach the TPC.

Since the transportation of neutrons should be modelled as precisely as possible, the simulation uses a Geant4 built-in physics list named `QGSP_BERT_HP` which has high-precision models for low-energy neutrons (below 20 MeV).

## 3 Digitisation and Analysis

Mokka writes out the energy deposits which happen during each single simulated step of a particle in the TPC volume (Figure 1). These steps are currently limited to a maximum length of 5 mm [7], which is a trade-off between accuracy and output file size. The energy deposits are afterwards assigned to discrete volume elements (so-called voxels), the sizes of which correspond to the size of the readout pads on the anode (in  $\rho$  and  $\phi$ ) and the readout sampling of the signals (in  $z$ ).

All 100 bunch crossings are overlaid with proper drift behaviour and bunch spacing, thereby forcing all signals into the “readout window” by a simple mod-

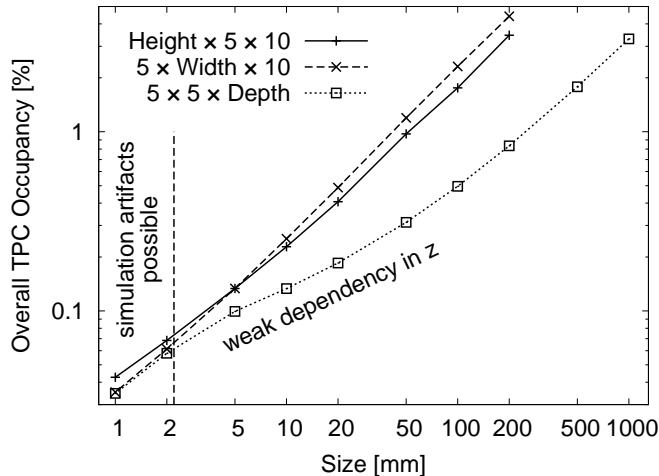


**Figure 2:** Occupancy in the TPC from 100 bunch crossings, calculated for different voxel sizes (note the logarithmic scale)

ulus operation – this should provide a sufficiently realistic picture from the middle of a long bunch train. (A few signals are created with very long delays, presumably because of nuclear reactions, but their fraction is negligibly small.) An ideal charge sharing over three pads is assumed, but  $z$ -dependent diffusion, gain fluctuations, or electronics effects such as shaping are not simulated yet.

### 3.1 Occupancy and Primary Space Charge

In Figure 2 the occupancy (i. e., the percentage of non-empty voxels) is calculated for different voxel sizes. Starting from  $5 \times 5 \times 10 \text{ mm}^3$ , the radial size (height of a pad row in  $\rho$ ), the azimuthal size (width of a pad in  $\phi$ ), and the longitudinal size (depth of a time bin in  $z$ ) are varied independently. The resulting overall occupancies stay well below 1% as long as the voxel dimensions do not get too large.

For height and width, the occupancy – as one would expect – scales almost linearly with the voxel size. However for the depth, there is only a weak dependency on the voxel size over a large domain. This is a consequence of the many microcurlers which travel a relatively long distance in  $z$ , but which only occupy very few pads in  $\rho$  and  $\phi$  (cf. Figure 1). Only when the voxel depth reaches approximately the size of the large curler structures, the corresponding curve in Figure 2 begins to rise as steeply as the other two. Even though this is irrelevant for a TPC (which would never have such a coarse longitudinal sampling), it might matter for other detector technologies.

Using the more-or-less realistic voxel size of  $5 \times 1 \times 10 \text{ mm}^3$ , Figure 3 shows that the local occupancy strongly depends on the radial position within the chamber. The innermost regions almost reach 1%, whereas in the middle and outer regions, occupancies of no more than 0.01% to 0.1% have to be expected.

The mean primary space charge ranges from almost  $10^{-3} \text{ fC/cm}^3$  in the inner regions down to approximately  $5 \cdot 10^{-5} \text{ fC/cm}^3$  in the middle and outer parts of the TPC. The distribution of the charge per voxel varies over a large range

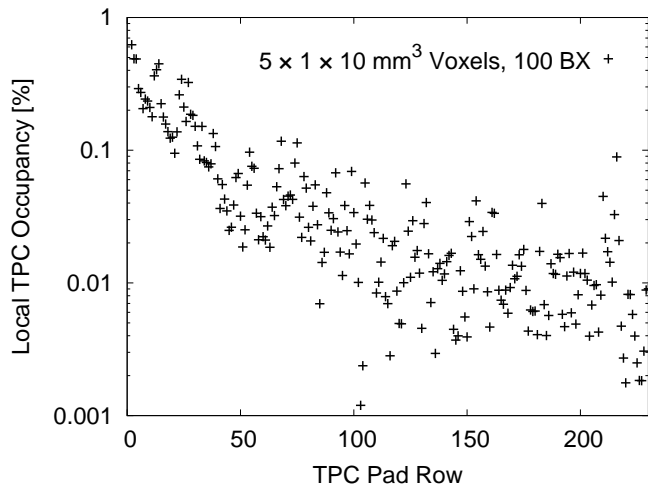


**Figure 3:** Local occupancy in the TPC from 100 bunch crossings, shown in dependence of the radial position

	5% CH <sub>4</sub>	20% CH <sub>4</sub>
Neutrons	142 ± 20	146 ± 25
Photons	947 ± 57	955 ± 44
Electrons	6 ± 13	6 ± 12
Electrons	292 ± 130	303 ± 121
Protons	2 ± 2	9 ± 4

**Table 1:** Number of particles which are entering the TPC (top part) and which are created in the TPC due to secondary processes (bottom part) per bunch crossing. The error values indicate the fluctuation per bunch crossing, not the total statistical error from all 100 bunch crossings.

(from a few primary electrons up to several thousands in the extreme case), but it does not follow a Landau-like shape due to the large contribution from photons which cause local energy deposits.

### 3.2 Influence of Neutrons and Hydrogen

It has been assumed that neutrons might have a significant influence on the TPC background by hitting protons and producing short recoil tracks, provided the chamber gas uses a quencher which contains hydrogen. To test this, another simulation run with 20% of CH<sub>4</sub> (instead of the usual 5%) is carried out. The results are shown in Table 1: One can in fact recognise a fourfold increase in signals created by protons (as far as the low statistics permits), but their fraction is negligible compared to the other ionisation processes. It should therefore be safe to use a conventional hydrocarbon-based quencher in typical concentrations instead of a surrogate which might introduce new kinds of problems.

## 4 Summary and Outlook

The occupancy of the TPC caused by machine-induced backgrounds stays well below the value of 1% which is often quoted as an approximate critical limit [8]. This single number still does not take the spatial structure of the background signals into account: Microcurlers will often blind only a few pads for a longer time. Such patterns will have less impact on data readout and pattern recognition than a set of truly randomly-distributed hits which might – numerically – yield the same value for the occupancy.

A pattern recognition algorithm should easily manage to remove most of these background signals before track finding and fitting, thus presumably minimising the direct influence on the tracker resolution as long as background levels do not get significantly higher. Furthermore, due to the strong radial dependency of the background occupancy, there will always be the option to start pattern recognition in the sparsely-populated outer regions of the TPC and then continue by tracking inwards.

However, background particles will still cause primary ionisation and possibly field distortions from backdrifting ions, thereby having at least an indirect influence on the performance of the tracker. These effects will have to be studied in further detail – a large-scale production of background events is foreseen for this purpose. Another plan is to include hadronic beamstrahlung scattering products (so-called minijets) in the simulations.

## References

- [1] Talk at the LCWS 2007, [ilcagenda.linearcollider.org/contributionDisplay.py?confId=1296&contribId=322](http://ilcagenda.linearcollider.org/contributionDisplay.py?confId=1296&contribId=322)
- [2] K. Yokoya, KEK Report 85-9 (1985).
- [3] D. Schulte, DESY Report TESLA 97-08 (1997).
- [4] ILC@SLAC Beam Parameters Web Site, [www-project.slab.stanford.edu/ilc/acceldev/beamparameters.html](http://www-project.slab.stanford.edu/ilc/acceldev/beamparameters.html)
- [5] Mokka Web Site, [mokka.in2p3.fr](http://mokka.in2p3.fr)
- [6] Large Detector Concept Web Site, [www.ilcldc.org](http://www.ilcldc.org)
- [7] A. Vogel, Simulation of a TPC for the ILC Detector, ILC Software and Physics Meeting, Cambridge, UK (2006), [ilcagenda.linearcollider.org/conferenceDisplay.py?confId=165](http://ilcagenda.linearcollider.org/conferenceDisplay.py?confId=165)
- [8] D. Kisielewska et al., Detector Outline Document for the Large Detector Concept (2006), [www.ilcldc.org/documents/dod/](http://www.ilcldc.org/documents/dod/)